Project NIGHT: Nuclear Isotopic Gas Hall Thruster

Joseph C. Thaggard[1], Jeffrey H. King[2], Luke Eister[3], Noble Shadowens[4], Andrew Crosson[5], Grayson Kunkel[6], Cameron Rodewald[7]
University of Alabama in Huntsville, Huntsville, AL, 35899, United States

This paper presents the preliminary research and simulation of a novel electric propulsion system utilizing existing Hall-effect thruster (HET) technology, nuclear electric propulsion (NEP) mission architecture, and small nuclear reactors (SNRs). The Nuclear Isotopic Gas Hall Thruster (NIGHT) utilizes fission reactor byproducts directly as propulsive fuel. A series of simulations is presented for reactor isotope generation, isotope decay, and transmutation. A second set of low-resolution simulations are run on the performance of the SPT-100 for in the "ideal mode" of Xe-135/Xe-136 and the "diesel mode" of direct isotope byproducts. A basic fuel management architecture is proposed to capture, store, and transmute reactor byproducts for improved efficiency against the "diesel mode" HET performance. Preliminary system elements are presented for further investigation.

I. Nomenclature

Σ_a = Macroscopic Absorption Cross-Section
σ_a = Microscopic Absorption Cross-Section
N = Atomic Number Density
φ = Neutron Flux
^{135}Xe = Xenon 135 Isotope
^{136}Xe = Xenon 136 Isotope
^{235}U = Uranium 235 Isotope

II. Introduction

Project Nuclear Isotopic Gas Hall Thruster (NIGHT) is a student-led research project at the University of Alabama in Huntsville. NIGHT investigates the use of isotopes created from a ^{235}U 10MW molten salt reactor (MSR) as a fuel source for a Hall-effect thruster (HET), primarily for station keeping and nuclear electric propulsion (NEP) attitude controls. The demand for use of electric propulsion devices for in-space use and subsequently the

[1] Undergraduate Student, Aerospace Engineering, Mechanical and Aerospace Department, Student Member. 1375686
[2] Undergraduate Student, Applied and Theoretical Physics, Science Department, Student Member. 1822414
[3] Undergraduate Student, Mechanical Engineering, Mechanical and Aerospace Department, Student Member. 115800
[4] Undergraduate Student, Applied and Theoretical Physics, Science Department, Student Member, 1927087
[5] Undergraduate Student, Aerospace Engineering, Mechanical and Aerospace Department, Student Member, 1927092
[6] Undergraduate Student, Aerospace Engineering, Mechanical and Aerospace Department, Student Member. 1845308
[7] Undergraduate Student, Mechanical Engineering, Mechanical and Aerospace Department, Student Member, 1810528

fuel for said devices has grown rapidly in the past years as a way to make an enclosed system. NIGHT theoretically uses undesirable byproduct isotopes for thrust, which would otherwise be expelled from the host vehicle.

III. Molten Salt Reactor (MSR) Performance and Simulation

The software OpenMC is used extensively to test and run simulations. 'OpenMC is a community-developed neutron and photon transport simulation code'[28] which was made in 2011 by members of the Computation Reactor Physics Group (CRPG) at MIT. The simulation software is capable of calculating fixed source, k-eigenvalue, and subcritical multiplications.

A. MSR Simulation

Several reactor configurations exist that are conceptually useful for isotope generation while remaining size efficient. From the literature reviews conducted, MSRs were the preferred option due to liquid fuel use compared to solid fuel reactors, such as boiling water reactors (BWR's), with MSRs having a better power density when compared to conventional reactors. In addition, more advanced fuel filtering and isotope extraction methods are available for MSRs versus BWRs. Within MSRs, fuel enrichment can largely determine the qualities of reactor performance. A highly enriched uranium (HEU) MSR reactor at 30% enrichment of ^{235}U was initially selected to determine if a higher enrichment would increase or decrease ^{135}Xe isotope production. Bateman Equations were used to establish the abundance of ^{135}Xe directly from fission events. Equation 1.1 and 1.2 relate the total power (T_p) to the energy released from fission (E_{Fiss}). Eq. (1.2) considers a 10MW reactor.

$$R_F = \frac{T_P}{E_{Fiss}} \tag{1.1}$$

$$R_F = \frac{10x10^6 W}{3.2x10^{-11} J} \Rightarrow R_F = 3.12x10^{17} Fiss/s \tag{1.2}$$

The fission reaction rate was found using Eq. 1.1 and Eq 1.2. A Bateman equation was solved to find the abundance of Iodine-135 (^{135}I), a precursor to ^{135}Xe. These concentrations also inform the selection of a gas sparging system, which removes the ^{135}Xe from the reactor fuel loop before a significant mass percent can decay. To allow for ^{135}Xe to be irradiated by neutrons, a secondary shield is simulated around the reactor core. This shield receives depositions of ^{135}Xe and assists in neutron absorption. Equations 2.1 and 2.2 describe the ^{135}I and ^{135}Xe Bateman equations, which considers the number of atoms (N), fission yield (γ), and decay constants (λ).

$$\frac{dN_{I135}}{dt} = \gamma_{I135} \cdot R_F - \lambda_{I135} \cdot N_{I135} \tag{2.1}$$

$$\frac{dN_{Xe135}}{dt} = \gamma_{Xe135} \cdot R_F + \lambda_{I135} \cdot N_{I135} - (\lambda_{Xe135} + \sigma_a \cdot \varphi_{core}) \cdot N_{Xe135} \tag{2.2}$$

From the Bateman equations above, a rate of $1.6e21$ atoms/day is achieved, which equates to 0.369 g/day of ^{135}Xe. Multiplying this by a sample mission period of 180 days, 66.4 g of ^{135}Xe is produced. While this isotope mass is useful, the MSR's geometry gives an advantage for transmuting ^{135}Xe into ^{136}Xe for further stability. This increases the neutron leakage rate by reducing the amount of fissile material encountered per comparable unit of length. An additional shield/storage chamber surrounds the core of the reactor, which is a mixture of shield water and ^{135}Xe, and further thermalizes neutrons for absorption or capture.

The geometry of this shield maximizes the neutron flux while performing radiation shielding functions. The dimensions are suggested from literature [30], with the values being: 4cm of steel, 31cm of H2O mixture or pure Xe, 4cm of steel, 8cm of lead, 4cm of steel. OpenMC takes the thickness of the shield into account when calculating the neutron leakage factor probability. OpenMC was used to calculate neutron leakage at multiple different enrichment values (10%, 15%, 20%, 30%, 37.5%). The graph below shows that without poisons in the core, which is an idealized scenario, the ideal enrichment would be between 10-20% ^{235}U.

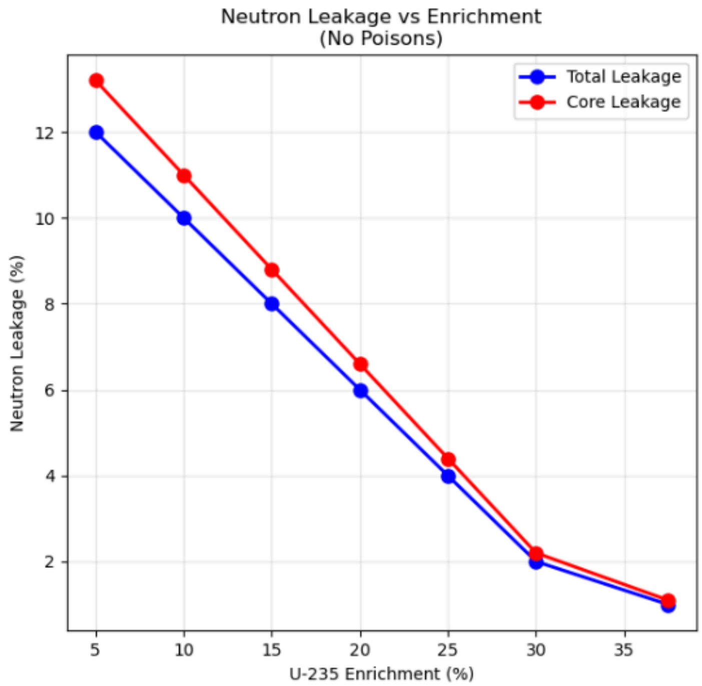

Figure 1: Neutron Leakage vs Enrichment in NIGHT reactor core.

Once the ^{135}Xe is harvested and put into one of the shield configurations (Water/ ^{135}Xe & pure ^{135}Xe), neutron flux can transmute ^{135}Xe into the stable ^{136}Xe for use in the HET.

$$L_{(e)} = 0.025 + \frac{(0.045-0.025)}{(1+(\frac{e}{15})^3} \tag{3}$$

$$f_{th(e)} = 0.15 + \frac{(0.65-0.15)}{(1+exp(\frac{(e-20)}{5})} \tag{4}$$

The shield ^{135}Xe storage chamber is made to mimic conventional reactor core shielding. Eq. (3) describes the neutron leakage. Eq. (4) calculates the fraction of thermal neutrons in the shield, which is ~70% ($3.6e10\frac{n}{cm^2}/s^2$). A code was made to track the ^{136}Xe production from ^{135}Xe transmutation, accounting for natural decay, absorption from pure ^{135}Xe, and absorption from ^{135}Xe mixed in water. Equation 5 describes the production process by neutron absorption.

$$^{135}Xe + n \rightarrow ^{136}Xe* \rightarrow ^{136}Xe + \gamma\,(8.4MeV) \tag{5}$$

Using OpenMC, the probability of ^{135}Xe absorbing a neutron can be solved using a simplified Bateman's equation with no fission source. A neutron absorption, as shown in Eq. (5), results in ^{136}Xe production. Equations 6.1, 6.2, and 6.3 describe the simplified Bateman's equations.

$$\frac{dN_{Xe135}}{dt} = -(\lambda_{Xe135} + K_{transmute})\, x\, N_{Xe135} \tag{6.1}$$

$$\frac{dN_{Xe136}}{dt} = K_{transmute}\ x\ N_{Xe135} \quad (6.2)$$

$$Where\ K_{transmute} = \sigma_{absorption}\ x\ \varphi_{shield} \quad (6.3)$$

With the aforementioned Bateman equations, the amount of ^{136}Xe produced over the mission period is found. A first study shown in Table 1 on enrichment variation is done to determine parameters for reactor optimization.

Enrichment (%)	**Thermal Flux ($\times 10^{10}$ n/cm²/s)**	**Xe-136 from Thermal (mg)**	**Xe-136 from Epithermal (mg)**	**Xe-136 from Fast (mg)**	**Total Xe-136 (mg)**	**Efficiency (%)**
10.0	4.8	12.8	1.4	0.2	14.4	0.019
15.0	3.6	9.8	1.1	0.1	11.0	0.017
20.0	2.7	6.9	0.8	0.1	7.8	0.014

Table 1: Xe-136 Production in H20/Xe-135 Shield

The pure ^{135}Xe shield table is not listed due to the minimal amounts of ^{136}Xe produced in said configuration.

The remaining 5% of ^{135}Xe present in the reactor can undergo transmutation via "burnup", which is related in Equation 7. Equation 7 relates the conversion fraction to burnup rate ($\sigma_a \phi$) with the ^{135}Xe decay constant (λ_{Xe135})

$$Conversion\ Fraction = \frac{\sigma_a \phi}{\sigma_a \phi + \lambda_{Xe135}} \quad (7)$$

Approximately 71.5% of ^{135}Xe absorbs a neutron and turns into ^{136}Xe in the core. If there is >95% harvest rate for ^{136}Xe, the total ^{136}Xe produced for use over the mission period is 2.281g.

Another two isotopes that can be used in a HET that are products of fission are Cesium-137 (^{137}Cs) and Krypton-85 (^{85}Kr). Their relatively long half-life ($t_{1/2}$) (^{137}Cs=30.17yrs, ^{85}Kr=10.76 years) allow them to be a viable option as a thruster fuel source. The amount of each isotope is found using Bateman equations for each isotope. Provided a harvest rate of 93% [16], Bateman equations find both isotopes' abundance from the core and compare abundance against various enrichment values, as seen in Table 2.

Enrich. (%)	**Fission Rate ($x10^{17}s^{-1}$)**	**Neutron Economy**	**Cs-137 Total (g)**	**Cs-137 (g/day)**	**Kr-85 Total (g)**	**Kr-85 (g/day)**	**Ba-137m (mg)**
10.0	3.43	0.850	74.9	0.414	0.004	0.00002	0.011
15.0	2.89	0.925	63.0	0.348	0.003	0.00002	0.010
20.0	2.14	0.980	46.8	0.259	0.002	0.00001	0.007

Table 2: Cs-137 & Kr-85 Production at different enrichment levels

With Table 1 and 2, if ^{137}Cs and ^{135}Xe production amounts over the mission period were to be combined, the total mass would be 129.4g over 180 days and 719 mg/day of fuel produced. The fission yields of these isotopes are consistent with the literature found [2] [3], which helps support the validity of the Bateman approach. The tables also show that changing enrichment parameters significantly impact isotope generation in the core. Table 3 notes the relationship between reactor power and isotope production using the Bateman approach detailed in this section.

Total Power (MWth)	Fission Rate (fissions/sec)	Neutron Economy	Xe-135 (g/180days)	Cs-137 (g/180days)	Kr-85 (g/180days)
10MWth	3.12e+17	0.0313	66.4	63.0	.003
100MWth	3.12e+18	0.0125	885.613	681.332	19.869

Table 3: Isotope Production in 10MW vs 100MW

Given the underlying logic remains unchanged, the code is updated with the values in Table 3. Increased power required larger reactor sizes, causing issues with the efficiency of sparging, which decreases due to core loop sizes increasing. This drop in efficiency will likely not be noticeable over the course of the mission. The ^{135}Xe decay chain also produces Cesium-135(^{135}Cs) through β^- decay, which has a $t_{1/2}$of 1.33e6 years. The long half-life effectively terminates the relevant decay chain for the purposes of the project.

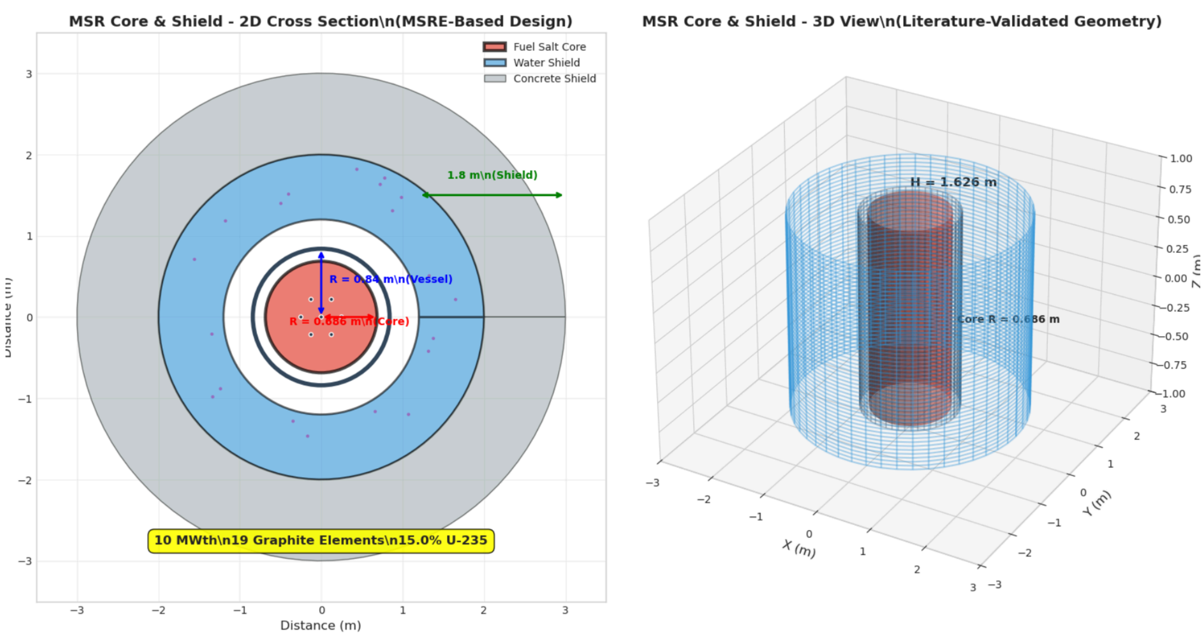

Figure 2: 3D Image of MSR Reactor

B. MSR Isotope Generation

Within a MSR, the fuel medium creates unique isotope decay dynamics. Fission products such as ^{135}Xe and ^{135}I are continuously created during ^{235}U fission; ^{135}I decays into ^{135}Xe via beta emission with a 6.6-hour half-life, and ^{135}Xe subsequently decays into ^{135}Cs with a 9.1-hour half-life [17]. Unlike solid-fuel reactors, MSRs are not "poisoned" by ^{135}Xe [10], as the liquid fuel allows for the continuous sparging of dissolved gaseous fission products [11]—reaching an estimated 95% removal efficiency. Furthermore, the flowing salt carries delayed neutron precursors out of the active core region, reducing their contribution to reactor kinetics [6]. Actinides such as ^{239}Pu, which is bred from ^{238}U via neutron capture and beta decay through ^{239}Np, also collect in the fuel salt.

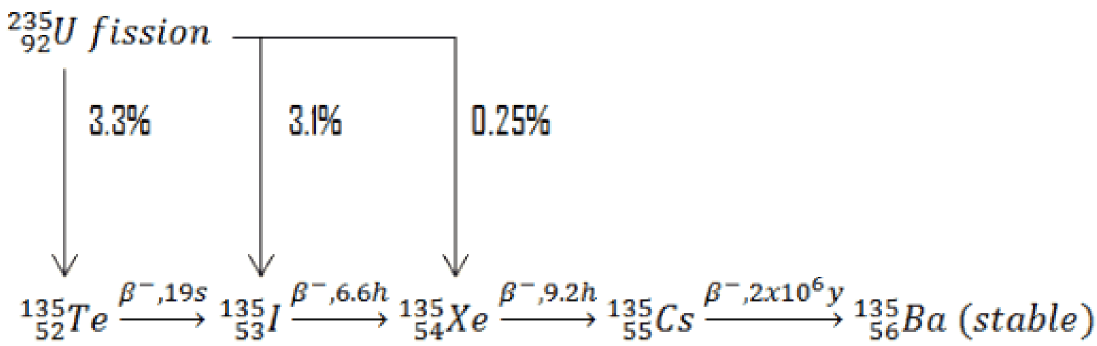

Figure 3: U-235 Fission Daughter Decay Chain (Te-135) [22]

IV. SPT-100 Thruster Simulations

Preliminary numerical simulations are required to determine the effectiveness of using reactor byproducts in a Hall thruster. This project utilizes HallThruster.jl, an open-source 1D fluid code designed for rapid performance estimation [21]. This tool was selected for its low computational overhead and reduced complexity compared to kinetic models or particle-in-cell (PIC) codes. The SPT-100 serves as the baseline model for this study, as its performance is well-documented and natively supported within the software [21]. Finally, specific cross-section data for each propellant must be incorporated, which can be derived from theoretical models or experimental databases.

C. Isotope Data.

Byproduct isotopes produced and recovered from the MSR reactor can vary greatly depending on reactor fuel enrichment, extraction method, and secondary irradiation. These isotope product decay chains include ^{135}Xe, ^{136}Xe, ^{85}Kr, and ^{137}Cs. These fuels would be the most likely to be used in an onboard electric propulsion system as their behaviors would dominate the net properties of the thruster plasma. HallThruster.jl requires cross-section data for every simulated propellant. To run a Hall thruster simulation, the following data ion sets are needed: ion excitation, ion elastic collision, +1/+2 excitation, +1/+3 excitation, +2/+3 excitation, 0/+1 excitation, 0/+2 excitation, and 0/+3 excitation. Traditionally, data for these sets are available on public databases such as Hayashi [26], Phelps [27], and others found in LXCat project [25]. For cross-sections and constants not available in LXCat, computational or approximate methods are available. The Lotz formula is an equation (Eq. 8) used to predict the excitation energies for any particle at any temperature, in electron-volts (eV) [29].

$$\sigma_{ion} = \sum_i a_i \frac{ln(E/I_i)}{EI_i} \tag{8}$$

σ_{ion} is the total cross-section for direct electron-ion impaction ionization in cm^2, E is the input energy in electron volts (eV), I_i is the ionization energy coefficient for the current subshell (eV), and a_i is the coefficient for that specific subshell.

In this case, all temperature dependent cross-sections are not dependent on atomic mass or atomic radius. As such, HallThruster.jl simulations can be produced with standard datasets or best approximations provided by the Lotz formula. However, atomic mass is considered an input condition for HallThruster.jl fuel class declarations, which allow for the isotope condition to be considered at lower simulation fidelity.

D. HallThurster.jl SPT-100 Light Xenon

The Stationary Plasma Thruster-100 (SPT-100) is a 1.35 kW Hall thruster first flown in 1993 [23]. This thruster has routinely been used as a benchmark for thruster performance simulations. The SPT-100 has ~80 mN thrust, 1600s of Isp, operates at 300 V, and consumes fuel at 5 mg/s [23]. HallThruster.jl uses this thruster as its regression test, providing a calibrated input set. To form a baseline performance, the SPT-100 simulation is run with Xenon-132 (^{132}Xe), where the average thrust and specific impulse were found to be about 92.67 mN and 1889s respectively.

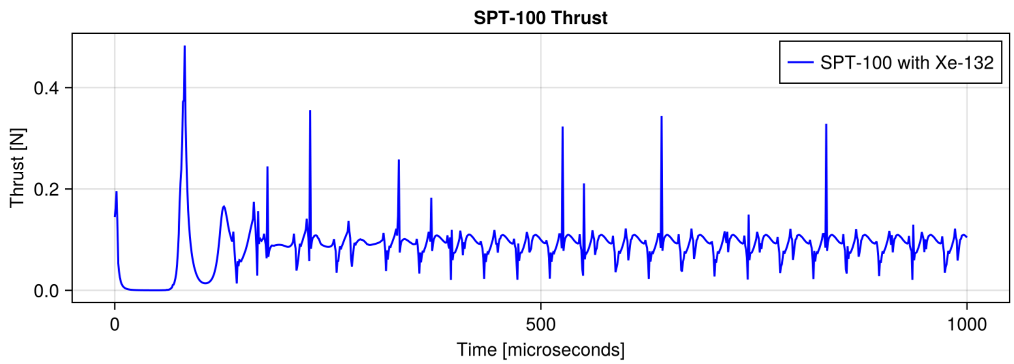

Figure 4: Baseline HallThruster.jl thrust results for the SPT-100 using standard Xe-132

E. SPT-100 "Diesel Mode" Simulation Feasibility

For the "diesel mode" simulation, the fuel is considered raw or unprocessed, better reflecting the fuel production rates seen naturally in an MSR reactor. These concentrations are simulated to test if multiple fuels can be effectively used in a Hall thruster despite chemical group and mass differences. HallThruster.jl has the capabilities to simulate both the heavier mass of the isotopic gas and propellants with multiple gasses. For these preliminary simulations, a standalone ^{135}Xe mode with a mass flow rate of 5 mg/s was run alongside an "unfinished diesel mode" consisting of both ^{135}Xe and ^{85}Kr with a mass flow rate ratio of 4:1 mg/s. Average thrust for the ^{135}Xe mode and unfinished diesel mode were found to be 91.56 mN and 93.11 mN respectively. Average specific impulse for the ^{135}Xe mode and unfinished diesel mode were found to be 1867s and 1898s respectively. At this time, the main bottleneck for fidelity is data availability for ^{137}Cs due to the complexity of solving the Lotz equation. The cross-sections required to produce the needed ionization coefficients are available but difficult to utilize.

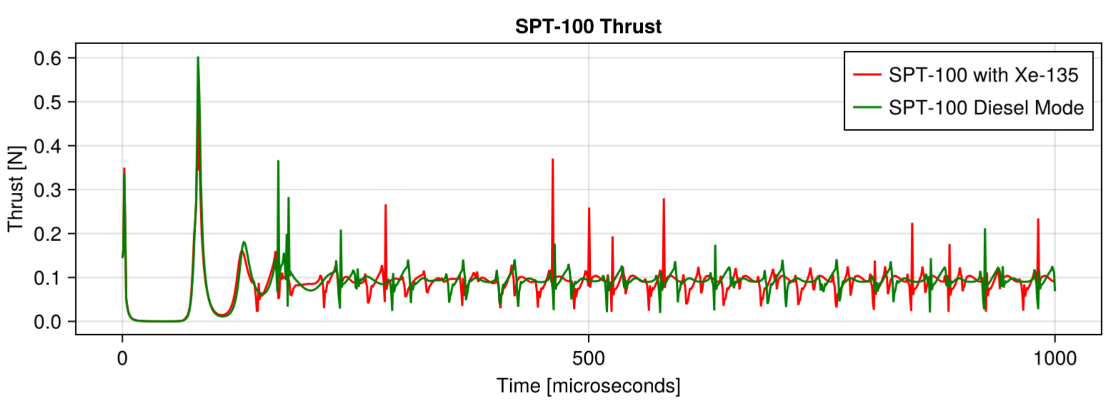

Figure 5: HallThruster.jl thrust results for the SPT-100 using Xe-135 and "Diesel Mode"

While these estimates are satisfactory for preliminary work, the radioactive effects of the propellants on the Hall thruster plasma and performance are not accounted for in this paper and in the literature. To accurately simulate thruster performance, stability, and breathing mode oscillations with these propellants using particle-in-cell codes, it is likely that predator-prey and kinetic models will have to be modified to account for decay energy deposition and the potential evolution of secondary electron emission if ^{137}Cs deposits on the discharge channel walls.

V. Fuel Management Architecture

F. Gas Sparging Technologies

The MSR is using a standard Off-Gas System (OGS) to remove the gaseous fission products and product daughters via gas sparging. The OGS employs helium as an inert carrier gas to facilitate degassing and sparging of the circulating fuel-salt mixture, thereby removing fission gases and other reactor-generated gaseous contaminants from the system [31]. Helium gas is injected directly into the primary coolant loop, near the pump exit. Curved vanes present in the separator will induce rotational velocity to the flow. The coolant quickly becomes saturated with dissolved helium, and thus more gas addition results in helium bubbles that allow the fission byproducts to diffuse into the helium bubbles [31]. Due to the concentration gradients between the helium bubbles and the dissolved gaseous fission products, this will then force the gaseous fission products to assimilate into the helium gas bubbles [24]. Therefore, gaseous fission products will form a true solution in salt, obeying the law of mass transfer (Henry's Law), shown in Equation 9. Henry's Law is sensitive to Henry's constant (k_h) and the current pressure (P).

$$C = k_h P \tag{9}$$

Since dissolved noble gasses form a true solution within the salt, the transport of the products should follow standard mass transfer laws, as shown in Equation 10 [24].

$$Mass\ Transfer\ Rate \propto (C_{actual} - C_0) \tag{10}$$

However, C_0 is roughly zero [24], this will allow the products to diffuse from the main salt line into the bubbles. The rotation of the fluid flow will cause the bubbles to drift towards the center of the extractor, where they are directed to a take-up line. The bubbles are then separated from the coolant, and the helium gas is separated from the gaseous fission products. The helium is then reused. All of the stripped gaseous products will then be redirected to a drain tank to store and further refine the products for use in a HET.

^{137}Cs is another isotope that can be reasonably harvested for usage. By operating the reactor at a temperature where the coolant flow is above the boiling point of cesium at the separator inlet, gaseous cesium isotopes can be removed using the same mechanisms as other gaseous fission products. Using new research [16] there is a theoretical way to separate both the solid and liquid forms that we should see in a MSR reactor. This new method is based on the solid-liquid equilibrium thermodynamics which states that cesium partitions preferentially between liquid and solid phases are based on thermodynamic stability. The equilibrium between phases is governed by equal chemical potentials, where at equilibrium the chemical potential of a given component is equal between the two phases, as shown in Eq. (11). Thermodynamic calculations indicated that a thermally controlled solid-liquid separation method holds the potential to recover up to 92.8% [16] of the initial cesium chloride.

$$\mu^{L_{cs}} = \mu^{S_{cs}} \tag{11}$$

$$a^{L_{cs}} \times \gamma^{L_{cs}} = a^{S_{cs}} \times \gamma^{S_{cs}} \tag{12}$$

It is noted that $\mu^{L_{cs}}$ is the liquid phase of cesium, while $\mu^{S_{cs}}$ is the solid phase, a is the current activity and γ is the activity coefficient. We can use the liquidus temperature (T_L) and solidus temperature (T_S) relationship to find the freezing range at which the separation window takes place.

VI. System Applications

There are few mission profiles that would prove a NIGHT thruster as practical. Such a mission would require an extremely large power demand, low yearly delta-V requirements, and long mission durations. Generally speaking, only outer planet exploration or space station orbital maintenance will be candidates for use of a NIGHT thruster. Early considerations for NIGHT applications included Jovian station orbital maintenance, L1 Lagrange station orbital maintenance, and NEP vehicle attitude controls.

G. NEP Vehicle Attitude Controls

The primary application considered for the NIGHT thruster is for vehicle orientation controls on a Nuclear Electric Propulsion (NEP) vehicle, as seen in modern literature [20]. NEP vehicles are the primary use case for this thruster due to their inherent nuclear power plant, relatively low vehicle mass, and long proposed mission durations. NEP vehicles utilize high-Isp and high-power electric propulsion systems to enable practical missions to the outer planets and Mars. Chemical propulsion or low-power electric propulsion traditionally struggles with reaching delta-V thresholds for outer planet exploration or cost-effective exploration of planets like Mars.

One of the highest-performing electric thrusters is Aerojet Rocketdyne's Advanced Electric Propulsion System (AEPS), which produces 600 mN thrust at 12 kW [18]. More advanced systems, such as magnetoplasmadynamic (MPD) thrusters, can promise single Newton performance at dozens of kilowatts [19]. As such, routine Mars missions or outer planet missions will likely carry high-performance nuclear reactors reaching into the MW power class, with 1 MW systems already under study. NEP missions have a variety of propulsive profiles to which the NIGHT thruster may be applicable. Chief among these is a "flip and burn" approach, where the NEP vehicle makes a burn to the Earth-Mars transfer orbit, then must rotate to point retrograde to begin decelerating for a capture orbit. The "flip" component can be performed by a series of NIGHT thrusters.

To calculate the effective performance for a NIGHT thruster, a simple MATLAB kinematic rotation script is written. Given the approximate dimensions of the ISS (reference vehicle), approximate moment of inertia, and a thruster performance of 80 mN (combined 320 mN for a bank of four thrusters) and 1600s of Isp, we establish a fuel mass to rotation time plot, as seen in Figure 6.

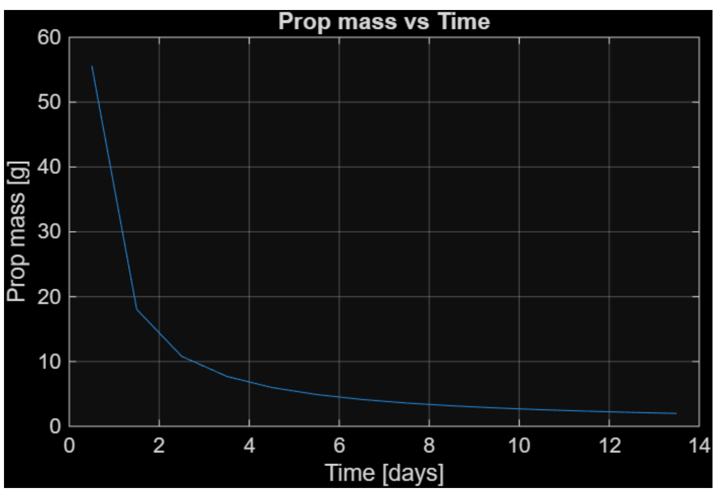

Figure 6: Fuel mass required for 180° rotation

The figure above shows that fuel required for an attitude control maneuver sharply decreases with rotation time. The smallest incitement of time allowed for a rotation was half a day. In previous OpenMC simulations, conservative reactor powers could produce enough fuel mass to allow for a control maneuver in the 60g range. This rotation is not practically noticeable by any onboard systems and the total thrust will place minimal mechanical strain on the NEP vehicle due to the limited thrust.

VII. Conclusions

Work for Project NIGHT has been highly successful in developing an initial model for an isotope-fueled Hall-effect thruster. An approximate model of a MSR was developed in OpenMC with custom shielding implemented to increase isotope production rates. A simple thruster performance model was developed and initial results are promising, with only a marginal decrease in performance metrics when compared to an industry standard thruster. An initial attitude control calculation revealed a potential pathway for NIGHT utilization. The work presented is highly preliminary, as all tools and analysis are low resolution. Future work will increase this resolution by introducing Monte-Carlo analysis, updated HET theory coupled with particle-in-cell (PIC) thruster analysis, and trajectory-specific attitude control.

VII. References

[1] Wigeland et al. (2016). 'Impact of thermal spectrum SMRs.' Ann. Nucl. Energy, 101

[2] Katcoff, S. & Rubinson, W. (1957). Yield of Kr-85 and Xe-133 in the thermal neutron fission of U-235. AEC Research and Development Report

[3] Brown, D.A. et al. (2018). ENDF/B-VIII.0: The 8th major release of the nuclear reaction data library. Nuclear Data Sheets, 148, 1-142.

[4] IAEA (2000). Compilation and evaluation of fission yield nuclear data. IAEA Technical Reports Series No. 371

[5] Mills, R. W. "Fission product yield evaluation." Annals of Nuclear Energy, vol. 22, no. 3, pp. 191-220, 1995.

[6] Robertson, R. C. "MSRE Design and Operations Report, Part I: Description of Reactor Design." Oak Ridge National Laboratory, ORNL-TM-732, 1965.

[7] Robertson, R. C., et al. "Conceptual Design Study of a Single-Fluid Molten-Salt Breeder Reactor." Oak Ridge National Laboratory, ORNL-4541, 1971

[8] U.S. Department of Energy. "Microreactor Program Objectives." Office of Nuclear Energy, DOE-NE-0210, 2020.

[9] Cetnar, J. "General solution of Bateman equations for nuclear transmutations." Annals of Nuclear Energy, vol. 33, no. 7, pp. 640-645, 2006.

[10] Weinberg, A. M., and E. P. Wigner. "The Physical Theory of Neutron Chain Reactors." University of Chicago Press, 1958. Chapter 9: Fission Product Poisoning.

[11] Watson, G. M., et al. "Behavior of noble gases in molten fluoride salt systems." Nuclear Applications, vol. 3, no. 8, pp. 488-492, 1967.

[12] Stacey, W. M. "Nuclear Reactor Physics." 3rd Edition, Wiley-VCH, 2018.

[13] McCoy, H. E., and J. R. Weir. "Materials development for molten-salt breeder reactors." Oak Ridge National Laboratory, ORNL-TM-1854, 1967.

[14] Nightingale, R. E., ed. "Nuclear Graphite." Academic Press, 1962.

[15] U.S. Department of Energy. "Molten Salt Reactor Campaign Implementation Plan." INL/EXT-20-57718, 2020.

[16] Rodríguez-Laguna, María del Rocío, et al. "Separation of fission products from high-level waste salt systems by partial crystallization: CsCl-NaCl-LiCl-KCl study." *Separation and Purification Technology*, vol. 332, 2024, p. 125602, doi:10.1016/j.seppur.2023.125602.

[17] Lamarsh, J. R., and A.J. Baratta. "Introduction to Nuclear Engineering." 3rd Edition, Prentice Hall, 2001.

[18] Herman, Daniel A., "Overview of the Development and Mission Application of the Advanced Electric Propulsion System (AEPS)", NASA/STI Accession number: 20180001297

[19] Cong, Yuntian., "The Experimental Performances of th1 100kW MPD Thruster with Applied Magnetic Field", 36th International Electric Propulsion Conference, IEPC-2019-310

[20] Mason, L., Oleson, S., Jacobson, D., Schmitz, P., Qualls, L., Smith, M., … Navarro, J. (2022). Nuclear Power Concepts and Development Strategies for High-Power Electric Propulsion Missions to Mars. Nuclear Technology, 208(sup1), S52–S66. https://doi.org/10.1080/00295450.2022.2045180

[21] Marks et al., (2023). HallThruster.jl: a Julia package for 1D Hall thruster discharge simulation. Journal of Open Source Software, 8(86), 4672, https://doi.org/10.21105/joss.04672

[22] Nuclear-Power.com, Iodine-135, https://www.nuclear-power.com/nuclear-power/reactor-physics/reactor-operation/xenon-135/iodine-135/

[23] Sankovic, John. M & Hamley, John. A, Performance of the Russian SPT-100 Thruster at NASA LeRC, 23rd International Electric Propulsion Conference, IEPC-93-094

[24] Valdez, P. J., Betzler, B. R., Wieselquist, W. A., & Fratoni, M. (2020). *Modeling molten salt reactor fission product removal with SCALE: Continuous depletion and removal framework* (ORNL/TM-2019/1418). Oak Ridge National Laboratory. https://info.ornl.gov/sites/publications/Files/Pub135162.pdf

[25] E. Carbone, W. Graef, G. Hagelaar, D. Boer, M.M. Hopkins, J.C. Stephens, B.T. Yee, S. Pancheshnyi, J. van Dijk, L. Pitchford, Data Needs for Modeling Low-Temperature Non-Equilibrium Plasmas: The LXCat Project, History, Perspectives and a Tutorial. Atoms (2021) 9 (1), 16.

[26] Hayashi database, www.lxcat.net, retrieved on February 24, 2026.

[27] Phelps database, www.lxcat.net, retrieved on February 24, 2026.

[28] OpenMC website, www.openmc.org

[29] Lotz, W. An empirical formula for the electron-impact ionization cross-section. Z. Physik 206, 205–211 (1967). https://doi.org/10.1007/BF01325928

[30] Robertson, R. C. "MSRE Design and Operations Report, Part I: Description of Reactor Design." *Oak Ridge National Laboratory*, ORNL-TM-732, 1965

[31] Gabbard, C. H. (1974). *Development of an axial-flow centrifugal gas bubble separator for use in MSR xenon removal system* (ORNL-TM-4533). Oak Ridge National Laboratory. https://www.osti.gov/servlets/purl/4324438